Nanostructured Columnar Tin Oxide Thin Film Electrode for Lithium Ion Batteries

Yuelan Zhang, Ying Liu, and Meilin Liu*

*Center for Innovative Fuel Cell and Battery Technologies, School of Materials Science and Engineering,
Georgia Institute of Technology, Atlanta, Georgia 30332-0245*

Nanostructured tin oxide thin films with columnar grains were deposited on gold-coated silicon substrates using the combustion chemical vapor deposition method. Microscopy revealed that the columnar grains were covered by nanoparticles of less than 20 nm. The electrochemical behavior of the as-prepared thin film electrodes was examined against a lithium counter electrode. These thin film electrodes exhibited high specific capacity and good capacity retention. The capacity increased from an initial value of about 353 (μA h)/(cm^2 μm) gradually to a maximum value of $\sim$490 (μA h)/(cm^2 μm) during cycling. The reversible capacity was about 460 (μA h)/(cm^2 μm) after 80 cycles at a charge/discharge rate of 0.3 mA/cm^2. When the electrodes were discharged at 0.9 mA/cm^2, the capacity retention obtained was about 64% of the capacity at 0.3 mA/cm^2. The good electrochemical performance is attributed to the unique nanostructure with longitudinal and radial connectivity of active materials.

Introduction

Tin oxide has been regarded as a potential substitute for commercial carbon-based materials due to its high storage capacity (781 (mA h)/g for tin dioxide vs 372 (mA h)/g for graphite). However, the large volume change (up to 300%) associated with alloying and de-alloying causes critical mechanical damage to the electrode, resulting in loss of capacity and rechargeability.[1−3] Potential solutions to the pulverization problem include modifying the material chemistry through doping, and designing novel and stable architectures using new fabrication techniques. In this paper, we report a tin oxide thin film electrode with nanostructured, columnar grains fabricated using a combustion chemical vapor deposition (CVD) process. The as-prepared SnO$_2$ electrode demonstrated high reversible capacity and excellent cyclability.

Prior investigations[4,5] suggested that the pulverization problems associated with the large volume difference between the lithiated and lithium-free host can be lessened by using a smaller particle (or small grain within these particles) morphology to reduce the absolute local volume changes of each reactive grain and by introducing a matrix (such as TCO[6]) to confine the volume change and reduce local mechanical stresses. Though the small particle size tin outperforms the coarse one, mobile Sn regions have the tendency to aggregate in a subsequent cycling process.[3,7] As

a result, the formation of large tin domains makes the material sensitive to cracking and crumbling, thus degenerating the capacity. Brousse et al.[8] reported that Li alloys would suffer from large Li-driven volume swings due to the growth of large clusters; and that the continuous percolation paths, and even worse the intergrain electronic contact across the composite, might also degrade electrode performance and cause electrode failure.

Recent investigations showed that nanostructured electrodes (e.g., nanotubes and nanowires) exhibited improved electrochemical behavior (e.g., superior rate capabilities and cyclability).[9−11] The performance of lithium ion battery electrodes could also be limited by mass transport of anions and cations through the bulk of the electrodes.[12,13] Mass transport limitations generally worsen the utilization and rate capability of electroactive materials,[14] while interfacial kinetics was dramatically facilitated by the high surface area of these nanostructured materials. Electrodes with open, porous, and connective architecture possess several features of interest in the design of novel battery materials, such as high accessible surface area, easy accessibility, connectivity of electroactive materials, and features on the nanometer scale.[15] The Li$^+$ diffusion distances are correspondingly

* To whom correspondence should be addressed. Phone: (404) 894-6114. Fax: (404) 894-9140. E-mail: meilin.liu@mse.gatech.edu.
(1) Besenhard, J. O.; Yang, J.; Winter, M. *J. Power Sources* **1997,** *68,* 87.
(2) Brousse, T.; Petoux, R.; Schleich, D. *J. Electrochem. Soc.* **1998,** *145,* 1.
(3) Courtney, I. A.; Dahn, J. R. *J. Electrochem. Soc.* **1997,** *144,* 2045.
(4) Winter, M.; Besenhard, J. O. *Electrochim. Acta* **1999,** *45,* 31.
(5) Courtney, I. A.; Dahn, J. R. *J. Electrochem. Soc.* **1997,** *144,* 2943.
(6) Idota, Y.; Kubota, T.; Matsufuji, A.; Maekawa, Y.; Miyasaka, T. *Science* **1997,** *276,* 1395.
(7) Courtney, I. A.; McKinnon, W. R.; Dahn, J. R. *J. Electrochem. Soc.* **1999,** *146,* 59.
(8) Brousse, T.; Paillard, P.; Retoux, R.; Schleich, D. M. *Proceedings of the 2nd Hawaii Battery Conference,* Big Island of Hawaii, Jan 4−7, 1999; p 294.
(9) Li, N.; Martin, C. R.; Scrosati, B. *Electrochem. Solid-State Lett.* **2000,** *3,* 316.
(10) (a) Li, N.; Patrissi, C. J.; Che, G.; Martin, C. R. *J. Electrochem. Soc.* **2000,** *147,* 2044. (b) Sides, C. R.; Martin, C. R. *Adv. Mater.* **2005,** *17,* 125.
(11) Fan, J.; Wang, T.; Yu, C.; Tu, B.; Jiang, Z.; Zhao, D. *Adv. Mater.* **2004,** *16,* 1432.
(12) Arora, P.; Doyle, M.; Gozdz, A. S.; White, R. E.; Newman, J. *J. Power Sources* **2000,** *88,* 219.
(13) Abraham, K. M.; Pasquariello, D. M.; Willstaedt, W. M. *J. Electrochem. Soc.* **1998,** *145,* 482.
(14) Scrosati, B. *J. Power Sources* **1994,** *51,* 79.

shorter, and the transport tortuosity is minimized;[16] hence, less time is needed to achieve full charge or discharge at the same current density. In addition, the larger surface areas of these electrode materials lower the local current density, resulting in a decrease of concentration polarization. Furthermore, assembly of the ultrafine electrode materials into continuous structures can enhance contacts and suppress free particle movement, so as to hinder aggregation of mobile electrode materials. Thus, the major challenge is to fabricate electrochemically active while structurally stable SnO_2 architectures. Here we report SnO_2 thin films with nanostructured columnar grains as negative electrodes for lithium ion batteries. The tin oxide thin films were deposited on gold-coated silicon substrates by a combustion CVD process. Combustion CVD is versatile in synthesis of nanostructured materials, which has been employed to prepare either nanosized powders or a variety of nanostructured ceramic films with controllable thickness and porosity for solid oxide fuel cells[17] and gas sensors.[18] SnO_2 thin films for lithium ion batteries deposited using combustion CVD are mechanically strong and electrochemically stable and demonstrate high reversible capacities.

Experimental Section

SnO_2 thin film electrodes were prepared by a combustion CVD process as described elsewhere.[17] Silicon substrates (4 mm × 4 mm) were then cut from a commercial 4 in. wafer. The Si substrates were then coated with gold for 10 min by dc sputtering. The precursor solution was prepared by dissolving tin(II) 2-ethylhexanoate (Aldrich) in absolute ethanol. The resulting solution was then pumped into a specially designed atomizer, where the precursor solution was mixed with high-pressure oxygen and atomized to produce a microscale mist. The solute-rich fine mist was combusted with the help of small CH_4/O_2 pilot flames. During deposition, the Au/Si(100) substrates were placed in the appropriate temperature zone of the combustion flame. Depositions were performed at 700 °C for 5 min. No additional annealing is needed for the as-deposited samples.

The crystallographic structure of the SnO_2 thin film was studied by X-ray powder diffraction (XRD) with Philips PW-1800 X-ray diffractometry at a scanning rate of 0.02 deg/min. The morphology of the as-deposited films was observed by scanning electron microscopy (SEM; Hitachi S-800).

A two-electrode cell configuration (Hohsen test cell, Hohsen Corp., Japan) was used for electrochemical measurements. The as-prepared SnO_2 film served as the working electrode. Copper foil, as a current collector, was mechanically attached to the backside of the silicon substrate. Lithium foil was used as the counter electrode. The electrolyte was a 50:50 (v/v) mixture of ethylene carbonate (EC) and diethyl carbonate (DEC) containing a 1 M solution of $LiPF_6$. All cells were assembled and tested in a glovebox (VAC) under a purified argon atmosphere. The electrochemical behaviors were measured by a Maccor battery test system (model 2300). The SnO_2 electrodes were galvanostatically charged (Li^+ insertion) and discharged (Li^+ extraction) in the voltage range of 0.1−1 V versus Li/Li^+, at a current density ranging from 100 to 900 $\mu A/cm^2$.

(15) Yan, H.; Sokolov, S.; Lytle, J. C.; Stein, A.; Zhang, F.; Smyrl, W. H. *J. Electrochem. Soc.* **2003**, *150*, A1102−A1107.
(16) Sakamoto, J. S.; Dunn, B. *J. Mater. Chem.* **2002**, *12*, 2859.
(17) Liu, Y.; Zha, S.; Liu, M. *Adv. Mater.* **2004**, *16*, 256.
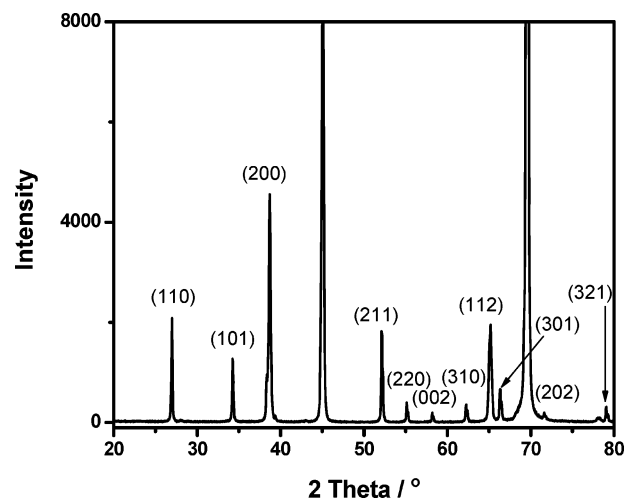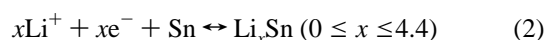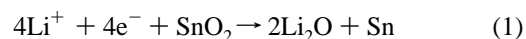(18) Liu, Y.; Koep, E.; Liu, M. *Chem. Mater.* **2005**, *17*, 3997.

Figure 1. XRD pattern of the as-prepared nanostructured tin oxide thin film.

Results and Discussion

Shown in Figure 1 is the X-ray diffraction pattern of the as-prepared tin oxide thin film on a Si substrate. The observed peaks correspond to a typical SnO_2 cassiterite phase (JCPDS 41-1445) except the two very sharp and intense peaks, which are attributed to the underneath Si(100) wafer. Au was not detected in the XRD spectra probably because the thickness of sputtered Au is under the detection limit.

Shown in Figure 2 are some typical SEM images of the nanostructured tin oxide thin film. As revealed in the side view (Figure 2a), the tin oxide film consisted of columnar grains of about 0.5−2 μm wide. The columnar grains grew from the substrate independently and separated from each other, leaving large spaces in between. The thickness of the film was about 5 μm. Figure 2b shows the top view of the tin oxide film. The inset is a higher magnification image, indicating the surface of each grain is covered by nanoparticles of less than 20 nm.

The as-prepared nanostructured tin oxide thin film was assembled into a test cell (against lithium) to evaluate the electrochemical performance. Shown in Figure 3 are the cell voltages of the first charging/discharging cycle as a function of the capacity of the nanostructured tin oxide thin film at a constant current density of 0.1 mA/cm^2. The galvanostatic charging and discharging experiments were conducted between potential limits of 0.1 and 1 V vs Li^+/Li. Prior to charge/discharge experiments, the electrodes were charged from the open-circuit potential to the lower potential limit of 0.1 V, and then discharged back to the upper limit of 1 V. The charge/discharge characteristic curve of the tin oxide thin film can be divided into two regions on the first charge curve: a typical irreversible plateau at 0.8−0.9 V in the first charge followed by a monotonic decrease to 0.1 V. The two-phase reaction in the tin oxide thin film can be described as follows:[3]

$$4Li^+ + 4e^- + SnO_2 \rightarrow 2Li_2O + Sn \tag{1}$$

$$xLi^+ + xe^- + Sn \leftrightarrow Li_xSn \ (0 \leq x \leq 4.4) \tag{2}$$

The two-step process involves a reduction of the tin oxide
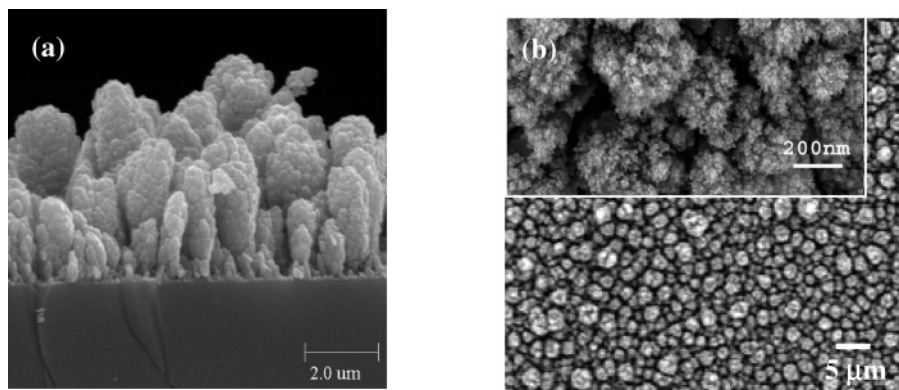
Figure 2. SEM images of the nanostructured tin oxide thin film: (a) side view and (b) top view. Insets are enlarged images.
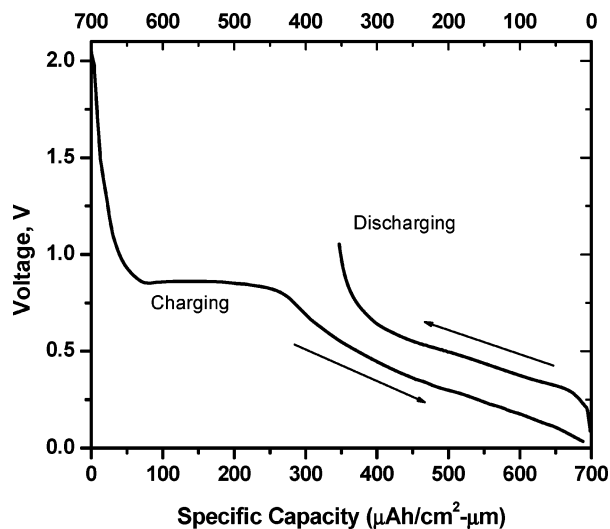

Figure 3. First potential profiles vs capacity of the nanostructured tin oxide thin film tested at a constant current density of 0.1 mA/cm^2.
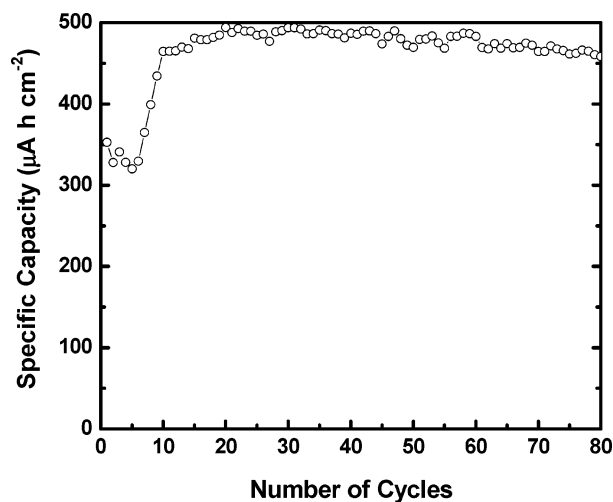

Figure 4. Discharge capacities vs number of charge/discharge cycles for the nanostructured tin oxide thin film. The charge/discharge rate is 0.3 mA/cm^2.

and lithium ion to metallic tin and lithium oxide and an alloying of the tin with lithium. The formation of the lithium oxide and metallic tin is an irreversible reaction responsible for the irreversible capacity in these systems. The reversible alloying and de-alloying processes offer reversible storage capacity. In the first charge/discharge process, the charge capacity was about 684 $(\mu A\ h)/(cm^2\ \mu m)$ and the discharge capacity was about 352.8 $(\mu A\ h)/(cm^2\ \mu m)$. The capacity loss of the initial charge/discharge was about 48%, which may be associated with the formation of a solid−electrolyte interface (SEI) layer on the surface of the tin oxide.

Figure 4 shows the discharge capacities vs the number of charge/discharge cycles at a constant rate of 0.3 mA/cm^2. The cycling behavior shows a progressive "activation" of the sample. There is a slight increase in capacity with increasing cycle numbers. The initial specific capacity was about 352.8 $\mu A/(cm^2\ \mu m)$, and was gradually increased to a maximum value of $\sim$490 $\mu A/(cm^2\ \mu m)$ after 20 cycles. The reversible capacity was maintained at about 460 $\mu A/(cm^2\ \mu m)$ after 80 cycles at a charge/discharge rate of 0.3 mA/cm^2. The discharging capacity retention was about 93%.

Summarized in Table 1 are the electrochemical properties of SnO$_2$ thin films prepared by different methods.[8,19−21] The reversible capacity of the nanostructured tin dioxide film

Table 1. Comparison of the Capacities of Various Tin Oxide Thin Films $((\mu A\ h)/(cm^2\ \mu m))$

| materials	preparation method	voltage range (V)	current density (mA/cm^2)	reversible capacity $((\mu A\ h)/(cm^2\ \mu m))$	ref
SnO$_2$	E-beam	0.1−0.8	0.1	200	19
Si−SnO$_2$	E-beam	0.1−0.8	0.1	302	19
SnOx	sputtering	0.01−1.4	0.1	498.33	20
SnO$_2$	sputtering	0.1−1.1	0.3	250	21
SnO$_2$	combustion CVD	0.1−1.0	0.3	352.77	this work

electrode prepared by combustion CVD is higher than those of electrodes prepared by other methods. Moreover, the cyclability of this film electrode is also very good.

Cycling tests were carried out at different current densities ranging from 0.3 to 0.9 mA/cm^2 over a voltage range of 0.1−1 V. As shown in Figure 5, lower capacities were observed at an increased discharge rate. For example, when the electrodes were discharged at a current density of 0.9 mA/cm^2, the capacity retention obtained was about 64% of the capacity at the current density of 0.3 mA/cm^2. It is worth noting that almost 100% capacity was retained when the charge/discharge rate was switched back to 0.3 mA/cm^2 after the capacity was tested at high rates for 60 cycles. The high

(19) Kim, Y.; Lee, W. H.; Moon, H.-S.; Ji, K. S.; Seong, S. H.; Park, J.-W. *J. Power Sources* **2001**, *101*, 353.

(20) Lee, W. H.; Son, H. C.; Moon, H. S.; Kim, Y. I.; Sung, S. H.; Kim, J. Y.; Lee, J. G.; Park, J. W. *J. Power Sources* **2000**, *89*, 102.

(21) Park, Y. J.; Park, K. S.; Kim, J. G.; Kim, M. K.; Kim, H. G.; Chung, H. T. *J. Power Sources* **2000**, *88*, 250.
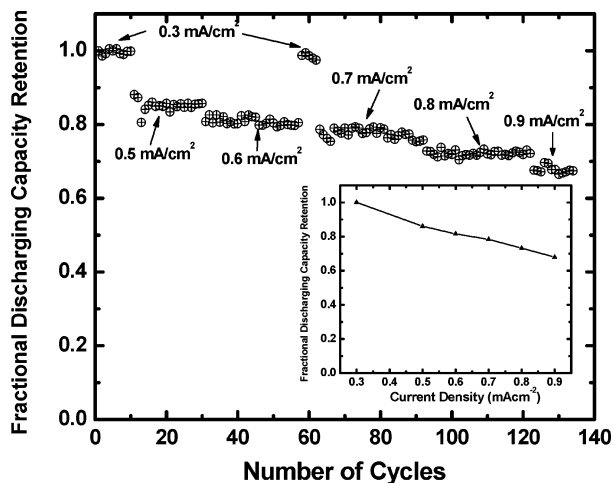
Figure 5. Dependence of the discharging capacity retention of the nanostructured tin dioxide thin film on the cycling rate and cycling numbers. The inset is the variation of the fractional discharging capacity retention with the discharge rate (continued after the cycle test shown in Figure 4).

capacity retention is attributed to the unique columnar morphology of the films with subtle nanosized features.

First, the tin oxide electrodes fabricated by combustion CVD are highly open and porous. It appears that each SnO_2 grain grew on top of the gold-coated Si substrate independently, with the growth rate much faster in the direction normal to the substrate surface, forming a columnar shape with wide, straight, and open voids between the grains. For porous films consisting of compacted nanoparticles, either poor interparticle contact or the tortuosity may make some portion of the particle surface electrochemically inactive. The columnar configuration of the films prepared by combustion CVD makes most of the grain surface readily accessible to liquid electrolyte. Larger accessible surface areas would lower the current density and decrease the possibility of local destruction of structure due to large Li^+ ion flux. Second, as shown in the inset of Figure 2b, the surface of columnar grains is covered by ultrafine particles of less than 20 nm. Fast surface lithium ion insertion−extraction interaction is expected. Third, this is essentially a three-dimensional electrode configuration for lithium ion batteries. The longitudinal connectivity of electroactive materials throughout the film thickness offers the additional advantage of fast electron/ion transport. The kinetic hindrance for lithium extraction depends not only on the Sn particle size but also on the architecture. Lithium transport is hindered by the slow transport kinetics of lithium from the bulk to the surface of the electroactive material particles. Fast transport kinetics would avoid ion depletion regions or concentration gradients that can degrade cell performance.[22,23] Especially at high charge/discharge rates, large Li^+ insertion or extraction fluxes at the surface and slow Li^+ transport in the bulk result in concentration polarization of Li^+ within the electrode material. The suitable ratio of surface area to thickness would improve the cell performance. Moreover, the gaps between column grains not only provide easy access of the surfaces to liquid electrolyte but also prevent agglomeration or growth of the grains, offering microstructural stability. Further, the uniformly distributed thin Li_2O film could also help accommodate the mechanical stress resulting from the large volume change during alloying and de-alloying cycles to maintain the structure integrity.

Conclusions

Three-dimensional SnO_2 anodes with nanostructured columnar grains were fabricated using a combustion CVD method. The thickness was readily controlled by the deposition time, varying typically from 1 to 5 μm. The as-prepared films demonstrated good electrochemical performance. The maximum obtainable reversible specific capacity of the tin oxide film was about 490 (μA h)/(cm^2 μm). More than 93% of the reversible capacity (460 (μA h)/(cm^2 μm)) was retained after 80 cycles at a current density of 0.3 mA/cm^2. More than 64% of the reversible capacity could be delivered at a discharge rate of 0.9 mA/cm^2. Combustion CVD has the potential to create unique electrode structures for high-performance lithium batteries.

(22) Owen, J. R. *Chem. Soc. Rev.* **1997,** *26*, 259.
(23) Patrissi, C. J.; Martin, C. R. *J. Electrochem. Soc.* **1999,** *146*, 3176.